MATCH
Communications in Mathematical and in Computer Chemistry

MATCH Commun. Math. Comput. Chem. **69** (2013) 333-354

ISSN 0340 - 6253

Restricted Enumerations by the Unit-Subduced-Cycle-Index (USCI) Approach. IV. The Restricted-Subduced-Cycle-Index (RSCI) Method for Enumeration of Kekulé Structures and of Perfect Matchings of Graphs

Shinsaku Fujita
Shonan Institute of Chemoinformatics and Mathematical Chemistry,
Kaneko 479-7 Ooimachi, Ashigara-Kami-Gun, Kanagawa-Ken,
258-0019 Japan
E-mail: shinsaku_fujita@nifty.com

(Received September 12, 2011)

Abstract

Restricted enumerations based on the unit-subduced-cycle-index (USCI) approach (S. Fujita, "Symmetry and Combinatorial Enumeration in Chemistry", Springer-Verlag (1991)) are discussed from a viewpoint of subductions into the $\mathbf{C}_1$-group, where only edges contained in a given skeleton are taken into consideration under a restriction condition that occupation of a common vertex (or occupation of adjacent edges) is avoided. The restriction condition for edge occupation is formulated by introducing territory indicators and territory discriminants so as to give a restricted subduced cycle index (RSCI) for the $\mathbf{C}_1$-group. Thereby, the restricted-subduced-cycle-index (RSCI) method for enumerating Kekulé structures (or equivalently perfect matchings of a graph) is developed as a specialized application of the USCI approach. To show the versatility of the RSCI method, the numbers of Kekulé structures for a dodecahedral skeleton, coronene, dibenzo[b,n]picene, dibenzo[bc,mn]ovalene, dibenzo[fg,op]anthanthrene, dibenzo[hi,sl]ovalene, naphtho[8,1,2-efg]anthanthrene, and fullerene C_{60} are calculated by the RSCI method. Maple programs for the RSCI method are reported as examples of practical calculations.

1 Introduction

Enumeration of Kekulé structures (or equivalently of perfect matchings of a given graph) is one of central problems of chemical graph theory. Various methods for enumerating Kekulé structures have been developed, as summarized in Chapter 8 of the textbook by Trinajstić [1], e.g., the method of fragmentation [2, 3], methods based on graphic polynomials such as the characteristic polynomial [4], the Gorden-Davisoson method [5], the numeral-in-hexagon method [6, 7], the method of Yen [8], the path counting method [9], the matrix method of Hall [10], the transfer-matrix method [11], and the Z-counting polynomial method [12].

In Parts II and III of this series, we have examined a problem on counting derivatives of a skeleton (e.g., a trigonal prismatic skeleton) under a restriction condition for vertex and edge substitution. A typical problem is described as follows:

> Consider the vertices and the edges of a skeleton as substitution sites. Suppose that achiral and chiral monodentate ligands are placed on the vertices (vertex substitution) and bidentate ligands are placed on the edges (edge substitution) *under the restriction condition that no occupation of common vertices (or no occupation of adjacent edges)* occurs. Evaluate the numbers of such derivatives.

As found easily, the restriction condition is equivalent to that of perfect matching, when we take account of edge substitution only, i.e., without considering vertex substitution. This implies that the methodology supporting the restricted FPM method of Part II and the restricted PCI method of Part III is applicable to enumerate perfect matchings (or Kekulé structures, chemically speaking).

The present paper is devoted to develop the restricted-subduced-cycle-index (RSCI) method for enumerating Kekulé structures as an extension of restricted enumerations based on the unit-subduced-cycle-index (USCI) approach.

2 Preliminaries

2.1 RSCIs for Symmetry-Itemized Enumeration of Kekulé Structures

For the purpose of examining Kekulé Structures or perfect matchings of graphs, only edge substitutions are taken into consideration. It follows that subduced cycle indices (SCIs without chirality fittingness) can be used in place of subduced cycle indices with chirality fittingness (SCI-CFs) (cf. Def. 19.3 of [13]). Thus, we start from Def. 15.1 of [13]:

$$\mathrm{SCI}(\mathbf{G}_j; s_{d_{jk}}^{(i\alpha)}) = \prod_{i=1}^{s} \prod_{\substack{\alpha=1 \\ \alpha_i \neq 0}}^{\alpha_i} \mathrm{Z}(\mathbf{G}(/\mathbf{G}_i) \downarrow \mathbf{G}_j; s_{d_{jk}}^{(i\alpha)}), \tag{1}$$

where $\mathrm{Z}(\mathbf{G}(/\mathbf{G}_i) \downarrow \mathbf{G}_j; s_{d_{jk}}^{(i\alpha)})$ is a unit subduced cycle index (USCI) for an orbit $\Delta_{i\alpha}$. For the notations of Eq. 1, see Chapter 15 of [13]. The definition of a territory discriminant of the SCI-CF (Def. 1 of Part II) is degenerated into the following definition of a territory discriminant of the SCI (Eq. 1) without considering chirality fittingness:

Definition 1 (Territory Discriminants for Respective Subgroups)

$$\mathrm{DSCI}(\mathbf{G}_j; s_{d_{jk}}^{(i\alpha)}, x_1, x_2, \ldots, x_v) = \prod_{i=1}^{s} \prod_{\substack{\alpha=1 \\ \alpha_i \neq 0}}^{\alpha_i} \mathrm{Z}(\mathbf{G}(/\mathbf{G}_i) \downarrow \mathbf{G}_j; s_{d_{jk}}^{(i\alpha)}) \Bigg|_{s_{d_{jk}}^{(i\alpha)} = 1 + s_{d_{jk}}^{(i\alpha)} t_{jk}^{(i\alpha)}(x_1, \ldots, x_v)} \tag{2}$$

for $j = 1, 2, \ldots s$. The symbol $t_{jk}^{(i\alpha)}(x_1, \ldots, x_v)$ denotes a territory indicator (TI) of the orbit $\Delta_{i\alpha}$, which is a product of dummy variables $x_1, x_2, \ldots, x_v$ corresponding to the terminal vertices (numbered as $1, 2, \ldots, v$) of edges contained in a suborbit (its sphericity index $s_{d_{jk}}^{(i\alpha)}$) of the orbit $\Delta_{i\alpha}$.

The expansion of Eq. 2 gives a set of candidate monomials (with TIs), among which monomials signified by a TI $x_1 x_2 \cdots x_v$ (in which each x_i appears only once) match the restriction condition and are necessary to construct a restricted SCI. The selection of such necessary monomials is accomplished by Lemma 1 of Part II of this series, which is degenerated into the following lemma by changing $\$_{d_{jk}}^{(i\alpha)}$ into $s_{d_{jk}}^{(i\alpha)}$ without considering chirality fittingness.

Lemma 1 (Restricted Subduced Cycle Indices (RSCIs)) Among the monomials contained in the territory discriminant generated by Def. 1, monomials signified by the TI $x_1 x_2 \cdots x_v$ (in which each x_i appears only once) are selected by means of the following equation:

$$\overline{\mathrm{SCI}}(\mathbf{G}_j; s_{d_{jk}}^{(i\alpha)}) = \frac{\partial^v}{\partial x_1 \partial x_2 \cdots \partial x_v} \mathrm{DSCI}(\mathbf{G}_j; s_{d_{jk}}^{(i\alpha)}, x_1, x_2, \ldots, x_v) \Bigg|_{x_1 = x_2 = \cdots = x_v = 0}, \tag{3}$$

where the TI part of each selected monomial is replaced by 1 (no appearance).

For example, let us consider a pyrene skeleton **1** shown in Fig. 1, where the numbering of vertices are arbitrarily selected.

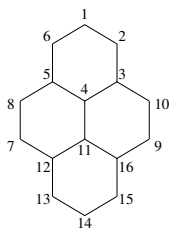

1

Figure 1: Numbering of a Pyrene Skeleton

The pyrene skeleton (**1**) belongs to $\mathbf{D}_{2h}$. The two-fold axes of subgroups $\mathbf{C}_2$, $\mathbf{C}_{2v}$, and $\mathbf{C}_{2h}$ are common, being perpendicular to the page at the midpoint of the edge $\{4, 11\}$. The two-fold axes of $\mathbf{C}'_2$, $\mathbf{C}'_{2v}$, and $\mathbf{C}'_{2h}$ are common, being contained in the page and running through the vertices 1, 4, 11, and 14. The two-fold axes of $\mathbf{C}''_2$, $\mathbf{C}''_{2v}$, and $\mathbf{C}''_{2h}$ are common, being contained in the page and running through the midpoints of the edges $\{7, 8\}$, $\{4, 11\}$, and $\{9, 10\}$. The

Table 1: Restricted SCIs for Pyrene

	SCI							Restricted SCI	
	full SCIs for orbits of edges						simplified	full	simplified
	$(\Delta_a$	Δ_b	Δ_c	Δ_d	Δ_e	$\Delta_f)$	SCI	RSCI	RSCI
$\mathbf{C}_1$	s_1	$\dot{s}_1^4$	$\tilde{\dot{s}}_1^4$	$\hat{\dot{s}}_1^4$	$\hat{\hat{\dot{s}}}_1^4$	$\dot{s}_1^2$	s_1^{19}	$2s_1\dot{s}_1^2\hat{\dot{s}}_1^2\hat{\hat{\dot{s}}}_1^2\dot{s}_1 + 4s_1^2\tilde{\dot{s}}_1^2\hat{\dot{s}}_1^2\dot{s}_1^2\dot{s}_1^2$	$6s_1^8$
$\mathbf{C}_2$	s_1	$\dot{s}_2^2$	$\tilde{\dot{s}}_2^2$	$\hat{\dot{s}}_2^2$	$\hat{\hat{\dot{s}}}_2^2$	$\dot{s}_2$	$s_1s_2^9$	$2\tilde{s}_2\tilde{\dot{s}}_2\hat{s}_2\dot{s}_2$	$2s_2^4$
$\mathbf{C}_2'$	s_1	$\dot{s}_2^2$	$\tilde{\dot{s}}_2^2$	$\hat{\dot{s}}_2^2$	$\hat{\hat{\dot{s}}}_2^2$	$\dot{s}_2$	$s_1s_2^9$	0	0
$\mathbf{C}_2''$	s_1	$\dot{s}_2^2$	$\tilde{\dot{s}}_2^2$	$\hat{\dot{s}}_2^2$	$\hat{\hat{\dot{s}}}_2^2$	$\dot{s}_1^2$	$s_1^3s_2^8$	$2s_1\tilde{s}_2\hat{s}_2\hat{\dot{s}}_2\dot{s}_1 + 2\tilde{s}_2\tilde{\dot{s}}_2\hat{s}_2\dot{s}_1^2$	$4s_1^2s_2^3$
$\mathbf{C}_s$	s_1	$\dot{s}_2^2$	$\tilde{\dot{s}}_2^2$	$\hat{\dot{s}}_2^2$	$\hat{\hat{\dot{s}}}_2^2$	$\dot{s}_2$	$s_1s_2^9$	0	0
$\mathbf{C}_s'$	s_1	$\dot{s}_2^2$	$\tilde{\dot{s}}_2^2$	$\hat{\dot{s}}_2^2$	$\hat{\hat{\dot{s}}}_2^2$	$\dot{s}_1^2$	$s_1^3s_2^8$	$2s_1\tilde{s}_2\hat{s}_2\hat{\dot{s}}_2\dot{s}_1 + 2\tilde{s}_2\tilde{\dot{s}}_2\hat{s}_2\dot{s}_1^2$	$4s_1^2s_2^3$
$\mathbf{C}_s''$	s_1	$\dot{s}_1^4$	$\tilde{\dot{s}}_1^4$	$\hat{\dot{s}}_1^4$	$\hat{\hat{\dot{s}}}_1^4$	$\dot{s}_1^2$	s_1^{19}	$2s_1\dot{s}_1^2\hat{\dot{s}}_1^2\hat{\hat{\dot{s}}}_1^2\dot{s}_1 + 4s_1^2\tilde{\dot{s}}_1^2\hat{\dot{s}}_1^2\dot{s}_1^2\dot{s}_1^2$	$6s_1^8$
$\mathbf{C}_i$	s_1	$\dot{s}_2^2$	$\tilde{\dot{s}}_2^2$	$\hat{\dot{s}}_2^2$	$\hat{\hat{\dot{s}}}_2^2$	$\dot{s}_2$	$s_1s_2^9$	$2\tilde{s}_2\tilde{\dot{s}}_2\hat{s}_2\dot{s}_2$	$2s_2^4$
$\mathbf{C}_{2v}$	s_1	$\tilde{s}_4$	$\tilde{\dot{s}}_4$	$\hat{s}_4$	$\hat{\hat{\dot{s}}}_4$	$\dot{s}_1^2$	$s_1s_2s_4^4$	0	0
$\mathbf{C}_{2v}'$	s_1	$\dot{s}_2^2$	$\tilde{\dot{s}}_2^2$	$\hat{\dot{s}}_2^2$	$\hat{\hat{\dot{s}}}_2^2$	$\dot{s}_2$	$s_1s_2^9$	0	0
$\mathbf{C}_{2v}''$	s_1	$\dot{s}_2^2$	$\tilde{\dot{s}}_2^2$	$\hat{\dot{s}}_2^2$	$\hat{\hat{\dot{s}}}_2^2$	$\dot{s}_1^2$	$s_1^3s_2^8$	$2s_1\tilde{s}_2\hat{s}_2\hat{\dot{s}}_2\dot{s}_1 + 2\tilde{s}_2\tilde{\dot{s}}_2\hat{s}_2\dot{s}_1^2$	$4s_1^2s_2^3$
$\mathbf{C}_{2h}$	s_1	$\dot{s}_2^2$	$\tilde{\dot{s}}_2^2$	$\hat{\dot{s}}_2^2$	$\hat{\hat{\dot{s}}}_2^2$	$\dot{s}_2$	$s_1s_2^9$	$2\tilde{s}_2\tilde{\dot{s}}_2\hat{s}_2\dot{s}_2$	$2s_2^4$
$\mathbf{C}_{2h}'$	s_1	$\tilde{s}_4$	$\tilde{\dot{s}}_4$	$\hat{s}_4$	$\hat{\hat{\dot{s}}}_4$	$\dot{s}_1^2$	$s_1s_2s_4^4$	0	0
$\mathbf{C}_{2h}''$	s_1	$\tilde{s}_4$	$\tilde{\dot{s}}_4$	$\hat{s}_4$	$\hat{\hat{\dot{s}}}_4$	$\dot{s}_1^2$	$s_1s_2s_4^4$	0	0
$\mathbf{D}_2$	s_1	$\tilde{s}_4$	$\tilde{\dot{s}}_4$	$\hat{s}_4$	$\hat{\hat{\dot{s}}}_4$	$\dot{s}_1^2$	$s_1s_2s_4^4$	0	0
$\mathbf{D}_{2h}$	s_1	$\tilde{s}_4$	$\tilde{\dot{s}}_4$	$\hat{s}_4$	$\hat{\hat{\dot{s}}}_4$	$\dot{s}_1^2$	$s_1s_2s_4^4$	0	0

mirror plane of $\mathbf{C}_s$ is perpendicular to the page and contains vertices 1, 4, 11, and 14. The mirror plane of $\mathbf{C}_s'$ is perpendicular to the page and contains the midpoints of the edges $\{7,8\}$, $\{4,11\}$, and $\{9,10\}$. The mirror plane of $\mathbf{C}_s''$ is a horizontal plane contained in the page.

The 19 edges of the pyrene skeleton (**1**) are divided into six orbits (Δ_a–Δ_f), which are respectively assigned to coset representations as follows:

$$\Delta_a = \{\{4,11\}\} \qquad \mathbf{D}_{2h}(/\mathbf{D}_{2h}) \quad \mathrm{Z}_a \tag{4}$$
$$\Delta_b = \{\{1,2\},\{1,6\},\{14,15\},\{13,14\}\} \qquad \mathbf{D}_{2h}(/\mathbf{C}_s'') \quad \mathrm{Z}_b \tag{5}$$
$$\Delta_c = \{\{3,4\},\{4,5\},\{11,12\},\{11,16\}\} \qquad \mathbf{D}_{2h}(/\mathbf{C}_s'') \quad \mathrm{Z}_c \tag{6}$$
$$\Delta_d = \{\{2,3\},\{5,6\},\{12,13\},\{15,16\}\} \qquad \mathbf{D}_{2h}(/\mathbf{C}_s'') \quad \mathrm{Z}_d \tag{7}$$
$$\Delta_e = \{\{3,10\},\{5,8\},\{7,12\},\{9,16\}\} \qquad \mathbf{D}_{2h}(/\mathbf{C}_s'') \quad \mathrm{Z}_e \tag{8}$$
$$\Delta_f = \{\{7,8\},\{9,10\}\} \qquad \mathbf{D}_{2h}(/\mathbf{C}_{2v}'') \quad \mathrm{Z}_f, \tag{9}$$

where each edge with terminal vertices k and l is represented by the symbol $\{k,l\}$. The six orbits (Δ_a–Δ_f) corresponds to respective USCIs as shown in Table 1, which are cited from [14]. The USCIs are differentiated by accent symbols in Table 1. The USCIs of each row (of a subgroup) are multiplied to give an SCI for the subgroup. For example, the $\mathbf{C}_1$-row shows the SCI, $s_1\dot{s}_1^4\tilde{\dot{s}}_1^4\hat{\dot{s}}_1^4\hat{\hat{\dot{s}}}_1^4\dot{s}_1^2$, in a full form of representation, which is simplified into s_1^{19} when the differentiation of suborbits are not taken into consideration.

According to Eq. 2 (Def. 1), the SCI $s_1\tilde{s}_1^4\tilde{\tilde{s}}_1^4\hat{s}_1^4\hat{\hat{s}}_1^4\dot{s}_1^2$ for $\mathbf{C}_1$ is transformed into the following territory discriminant:

$$\begin{aligned}
&\mathrm{DSCI}(\mathbf{C}_1; s_d, \tilde{s}_d, \ldots, x_1, x_2, \ldots, x_v) \\
&= (1+s_1x_4x_{11}) \\
&\quad \times (1+\tilde{s}_1x_1x_2)(1+\tilde{s}_1x_1x_6)(1+\tilde{s}_1x_{14}x_{15})(1+\tilde{s}_1x_{13}x_{14}) \\
&\quad \times (1+\tilde{\tilde{s}}_1x_3x_4)(1+\tilde{\tilde{s}}_1x_4x_5)(1+\tilde{\tilde{s}}_1x_{11}x_{12})(1+\tilde{\tilde{s}}_1x_{11}x_{16}) \\
&\quad \times (1+\hat{s}_1x_2x_3)(1+\hat{s}_1x_5x_6)(1+\hat{s}_1x_{12}x_{13})(1+\hat{s}_1x_{15}x_{16}) \\
&\quad \times (1+\hat{\hat{s}}_1x_3x_{10})(1+\hat{\hat{s}}_1x_5x_8)(1+\hat{\hat{s}}_1x_7x_{12})(1+\hat{\hat{s}}_1x_9x_{16}) \\
&\quad \times (1+\dot{s}_1x_7x_8)(1+\dot{s}_1x_9x_{10}),
\end{aligned} \tag{10}$$

where respective rows of the right-hand side correspond to the orbits shown as Δ_a–Δ_f (Eqs. 4–9). Note that Eq. 10 is effective to $\mathbf{C}_s''$.

Similarly, the other SCIs collected in Table 1 are transformed into corresponding territory discriminants as follows:

$$\begin{aligned}
\mathrm{DSCI}(\mathbf{C}_2; s_d, \tilde{s}_d, \ldots, x_1, x_2, \ldots, x_v) &= (1+s_1x_4x_{11}) \\
&\quad \times (1+\tilde{s}_2x_1x_2x_{13}x_{14})(1+\tilde{s}_2x_1x_6x_{14}x_{15}) \\
&\quad \times (1+\tilde{\tilde{s}}_2x_3x_4x_{11}x_{12})(1+\tilde{\tilde{s}}_2x_4x_5x_{11}x_{16}) \\
&\quad \times (1+\hat{s}_2x_2x_3x_{12}x_{13})(1+\hat{s}_2x_5x_6x_{15}x_{16}) \\
&\quad \times (1+\hat{\hat{s}}_2x_3x_{10}x_7x_{12})(1+\hat{\hat{s}}_2x_5x_8x_9x_{16}) \\
&\quad \times (1+\dot{s}_2x_7x_8x_9x_{10})
\end{aligned} \tag{11}$$

$$\begin{aligned}
\mathrm{DSCI}(\mathbf{C}_2'; s_d, \tilde{s}_d, \ldots, x_1, x_2, \ldots, x_v) &= (1+s_1x_4x_{11}) \\
&\quad \times (1+\tilde{s}_2x_1x_2x_1x_6)(1+\tilde{s}_2x_13x_{14}x_{14}x_{15}) \\
&\quad \times (1+\tilde{\tilde{s}}_2x_3x_4x_4x_5)(1+\tilde{\tilde{s}}_2x_11x_12x_{11}x_{16}) \\
&\quad \times (1+\hat{s}_2x_2x_3x_5x_6)(1+\hat{s}_2x_{12}x_{13}x_{15}x_{16}) \\
&\quad \times (1+\hat{\hat{s}}_2x_3x_{10}x_5x_8)(1+\hat{\hat{s}}_2x_7x_{12}x_9x_{16}) \\
&\quad \times (1+\dot{s}_2x_7x_8x_9x_{10})
\end{aligned} \tag{12}$$

$$\begin{aligned}
\mathrm{DSCI}(\mathbf{C}_2''; s_d, \tilde{s}_d, \ldots, x_1, x_2, \ldots, x_v) &= (1+s_1x_4x_{11}) \\
&\quad \times (1+\tilde{s}_2x_1x_2x_{14}x_{15})(1+\tilde{s}_2x_1x_6x_{13}x_{14}) \\
&\quad \times (1+\tilde{\tilde{s}}_2x_3x_4x_{11}x_{16})(1+\tilde{\tilde{s}}_2x_4x_5x_{11}x_{12}) \\
&\quad \times (1+\hat{s}_2x_2x_3x_{15}x_{16})(1+\hat{s}_2x_5x_6x_{12}x_{13}) \\
&\quad \times (1+\hat{\hat{s}}_2x_3x_{10}x_9x_{16})(1+\hat{\hat{s}}_2x_5x_8x_7x_{12}) \\
&\quad \times (1+\dot{s}_1x_7x_8)(1+\dot{s}_1x_9x_{10})
\end{aligned} \tag{13}$$

$$\begin{aligned}
&= (1+s_1x_4x_11) \\
&\quad \times (1+\tilde{s}_4x_1x_2x_{14}x_{15}x_1x_6x_{13}x_{14}) \\
&\quad \times (1+\tilde{\tilde{s}}_4x_3x_4x_{11}x_{16}x_4x_5x_{11}x_{12}) \\
&\quad \times (1+\hat{s}_4x_2x_3x_{15}x_{16}x_5x_6x_{12}x_{13}) \\
&\quad \times (1+\hat{\hat{s}}_4x_3x_{10}x_5x_8x_7x_{12}x_9x_{16}) \\
&\quad \times (1+\dot{s}_2x_7x_8x_9x_{10})
\end{aligned} \tag{14}$$

Note that Eq. 11 is effective to $\mathbf{C}_i$ and $\mathbf{C}_{2h}$; Eq. 12 is effective to $\mathbf{C}_s$ and $\mathbf{C}_{2v}'$; Eq. 13 is effective to $\mathbf{C}_s'$ and $\mathbf{C}_{2v}''$; as well as Eq. 14 is effective to $\mathbf{C}_{2h}'$, $\mathbf{C}_{2h}''$ $\mathbf{D}_2$, and $\mathbf{D}_{2h}$.

According to Eq. 3 (Lemma 1), Eqs. 10–14 are treated to give the corresponding restricted subduced cycle indices (RSCIs). For example, the RSCI for $\mathbf{C}_1$ is calculated by the following program (named "pyreneRSCI-A), which is programmed by using the Maple programming language [15].

```
#pyreneRSCI-A.mpl
DSCIC1 :=
(1+s1*x4*x11)*
(1+ss1*x1*x2)*(1+ss1*x1*x6)*(1+ss1*x14*x15)*(1+ss1*x13*x14)*
(1+S1*x3*x4)*(1+S1*x4*x5)*(1+S1*x11*x12)*(1+S1*x11*x16)*
(1+SS1*x2*x3)*(1+SS1*x5*x6)*(1+SS1*x12*x13)*(1+SS1*x15*x16)*
(1+SSS1*x3*x10)*(1+SSS1*x5*x8)*(1+SSS1*x7*x12)*(1+SSS1*x9*x16)*
(1+sss1*x7*x8)*(1+sss1*x9*x10);

tempC1A := expand(DSCIC1):
tempC1B := diff(tempC1A, x1,x2,x3,x4,x5,x6,x7,x8,
x9,x10,x11,x12,x13,x14,x15,x16):

x1 :=0; x2 :=0; x3 :=0; x4 :=0; x5 :=0;
x6 :=0; x7 :=0; x8 :=0; x9 :=0; x10 :=0;
x11 :=0; x12 :=0; x13 :=0; x14 :=0; x15 :=0; x16 :=0;

resSCIC1 := expand(tempC1B);
```

In this source list, `s1` stands for s_1, `ss1` stands for $\tilde{s}_1$, `S1` stands for $\tilde{\tilde{s}}_1$, `SS1` stands for $\hat{s}_1$, `SSS1` stands for $\hat{\hat{s}}_1$, and `sss1` stands for $\dot{s}_1$. The execution of this program by the Maple system generates the following result:

$$\overline{\mathrm{SCI}}(\mathbf{C}_1;s_d,\tilde{s}_d,\ldots) = 2s_1\tilde{s}_1^2\tilde{\tilde{s}}_1^2\hat{\hat{s}}_1^2\dot{s}_1 + 4\tilde{s}_1^2\tilde{\tilde{s}}_1^2\hat{s}_1^2\dot{s}_1^2. \tag{15}$$

The other RSCIs for respective subgroups are calculated in similar ways and collected in the full-RSCI column of Table 1.

According to Def. 1 of Part III of this series, the restricted SCIs collected in the full-RSCI column of Table 1 and the inverse mark table of $\mathbf{D}_{2h}$ [14] give the following set of restricted PCIs (RPCIs):

$$\begin{aligned}
\overline{\mathrm{PCI}}(\mathbf{C}_1;s_d,\tilde{s}_d,\ldots) &= \frac{1}{8}\overline{\mathrm{SCI}}(\mathbf{C}_1;s_d,\tilde{s}_d,\ldots) - \frac{1}{8}\overline{\mathrm{SCI}}(\mathbf{C}_2;s_d,\tilde{s}_d,\ldots) \\
&\quad - \frac{1}{8}\overline{\mathrm{SCI}}(\mathbf{C}_2';s_d,\tilde{s}_d,\ldots) - \frac{1}{8}\overline{\mathrm{SCI}}(\mathbf{C}_2'';s_d,\tilde{s}_d,\ldots) \\
&\quad - \frac{1}{8}\overline{\mathrm{SCI}}(\mathbf{C}_s;s_d,\tilde{s}_d,\ldots) - \frac{1}{8}\overline{\mathrm{SCI}}(\mathbf{C}_s';s_d,\tilde{s}_d,\ldots) \\
&\quad - \frac{1}{8}\overline{\mathrm{SCI}}(\mathbf{C}_s'';s_d,\tilde{s}_d,\ldots) - \frac{1}{8}\overline{\mathrm{SCI}}(\mathbf{C}_i;s_d,\tilde{s}_d,\ldots) \\
&\quad + \frac{1}{4}\overline{\mathrm{SCI}}(\mathbf{C}_{2v};s_d,\tilde{s}_d,\ldots) + \frac{1}{4}\overline{\mathrm{SCI}}(\mathbf{C}_{2v}';s_d,\tilde{s}_d,\ldots) \\
&\quad + \frac{1}{4}\overline{\mathrm{SCI}}(\mathbf{C}_{2v}'';s_d,\tilde{s}_d,\ldots) + \frac{1}{4}\overline{\mathrm{SCI}}(\mathbf{C}_{2h};s_d,\tilde{s}_d,\ldots) \\
&\quad + \frac{1}{4}\overline{\mathrm{SCI}}(\mathbf{C}_{2h}';s_d,\tilde{s}_d,\ldots) + \frac{1}{4}\overline{\mathrm{SCI}}(\mathbf{C}_{2h}'';s_d,\tilde{s}_d,\ldots) \\
&\quad + \frac{1}{4}\overline{\mathrm{SCI}}(\mathbf{D}_2';s_d,\tilde{s}_d,\ldots) - \overline{\mathrm{SCI}}(\mathbf{D}_{2h};s_d,\tilde{s}_d,\ldots) \\
&= 0
\end{aligned} \tag{16}$$

$$\begin{aligned}
\overline{\mathrm{PCI}}(\mathbf{C}_2;s_d,\tilde{s}_d,\ldots) &= \frac{1}{4}\overline{\mathrm{SCI}}(\mathbf{C}_2;s_d,\tilde{s}_d,\ldots)-\frac{1}{4}\overline{\mathrm{SCI}}(\mathbf{C}_{2v};s_d,\tilde{s}_d,\ldots)\\
&\quad -\frac{1}{4}\overline{\mathrm{SCI}}(\mathbf{C}_{2y};s_d,\tilde{s}_d,\ldots)-\frac{1}{4}\overline{\mathrm{SCI}}(\mathbf{D}_2;s_d,\tilde{s}_d,\ldots)\\
&\quad +\frac{1}{2}\overline{\mathrm{SCI}}(\mathbf{D}_{2h};s_d,\tilde{s}_d,\ldots)=0 \qquad (17)\\
\overline{\mathrm{PCI}}(\mathbf{C}_2';s_d,\tilde{s}_d,\ldots) &= \frac{1}{4}\overline{\mathrm{SCI}}(\mathbf{C}_2';s_d,\tilde{s}_d,\ldots)-\frac{1}{4}\overline{\mathrm{SCI}}(\mathbf{C}_{2v}';s_d,\tilde{s}_d,\ldots)\\
&\quad -\frac{1}{4}\overline{\mathrm{SCI}}(\mathbf{C}_{2h}';s_d,\tilde{s}_d,\ldots)-\frac{1}{4}\overline{\mathrm{SCI}}(\mathbf{D}_2;s_d,\tilde{s}_d,\ldots)\\
&\quad +\frac{1}{2}\overline{\mathrm{SCI}}(\mathbf{D}_{2h};s_d,\tilde{s}_d,\ldots)=0 \qquad (18)\\
\overline{\mathrm{PCI}}(\mathbf{C}_2'';s_d,\tilde{s}_d,\ldots) &= \frac{1}{4}\overline{\mathrm{SCI}}(\mathbf{C}_2'';s_d,\tilde{s}_d,\ldots)-\frac{1}{4}\overline{\mathrm{SCI}}(\mathbf{C}_{2v}'';s_d,\tilde{s}_d,\ldots)\\
&\quad -\frac{1}{4}\overline{\mathrm{SCI}}(\mathbf{C}_{2h}'';s_d,\tilde{s}_d,\ldots)-\frac{1}{4}\overline{\mathrm{SCI}}(\mathbf{D}_2;s_d,\tilde{s}_d,\ldots)\\
&\quad +\frac{1}{2}\overline{\mathrm{SCI}}(\mathbf{D}_{2h};s_d,\tilde{s}_d,\ldots)=0 \qquad (19)\\
\overline{\mathrm{PCI}}(\mathbf{C}_s;s_d,\tilde{s}_d,\ldots) &= \frac{1}{4}\overline{\mathrm{SCI}}(\mathbf{C}_s;s_d,\tilde{s}_d,\ldots)-\frac{1}{4}\overline{\mathrm{SCI}}(\mathbf{C}_{2v};s_d,\tilde{s}_d,\ldots)\\
&\quad -\frac{1}{4}\overline{\mathrm{SCI}}(\mathbf{C}_{2v}'';s_d,\tilde{s}_d,\ldots)-\frac{1}{4}\overline{\mathrm{SCI}}(\mathbf{C}_{2h}'';s_d,\tilde{s}_d,\ldots)\\
&\quad +\frac{1}{2}\overline{\mathrm{SCI}}(\mathbf{D}_{2h};s_d,\tilde{s}_d,\ldots)=0 \qquad (20)\\
\overline{\mathrm{PCI}}(\mathbf{C}_s';s_d,\tilde{s}_d,\ldots) &= \frac{1}{4}\overline{\mathrm{SCI}}(\mathbf{C}_s';s_d,\tilde{s}_d,\ldots)-\frac{1}{4}\overline{\mathrm{SCI}}(\mathbf{C}_{2v};s_d,\tilde{s}_d,\ldots)\\
&\quad -\frac{1}{4}\overline{\mathrm{SCI}}(\mathbf{C}_{2v}'';s_d,\tilde{s}_d,\ldots)-\frac{1}{4}\overline{\mathrm{SCI}}(\mathbf{C}_{2h}';s_d,\tilde{s}_d,\ldots)\\
&\quad +\frac{1}{2}\overline{\mathrm{SCI}}(\mathbf{D}_{2h};s_d,\tilde{s}_d,\ldots)=0 \qquad (21)\\
\overline{\mathrm{PCI}}(\mathbf{C}_s'';s_d,\tilde{s}_d,\ldots) &= \frac{1}{4}\overline{\mathrm{SCI}}(\mathbf{C}_s'';s_d,\tilde{s}_d,\ldots)-\frac{1}{4}\overline{\mathrm{SCI}}(\mathbf{C}_{2v}';s_d,\tilde{s}_d,\ldots)\\
&\quad -\frac{1}{4}\overline{\mathrm{SCI}}(\mathbf{C}_{2v}'';s_d,\tilde{s}_d,\ldots)-\frac{1}{4}\overline{\mathrm{SCI}}(\mathbf{C}_{2h};s_d,\tilde{s}_d,\ldots)\\
&\quad +\frac{1}{2}\overline{\mathrm{SCI}}(\mathbf{D}_{2h};s_d,\tilde{s}_d,\ldots)\\
&= \frac{1}{2}s_1\tilde{s}_1^2\hat{s}_1^2\hat{\dot{s}}_1^2\dot{s}_1+\tilde{s}_1^2\tilde{\dot{s}}_1^2\hat{s}_1^2\dot{s}_1^2-\frac{1}{2}s_1\tilde{s}_2\hat{s}_2\hat{\dot{s}}_2\dot{s}_1\\
&\quad -\frac{1}{2}\tilde{s}_2\tilde{\dot{s}}_2\hat{s}_2\dot{s}_1^2-\frac{1}{2}\tilde{s}_2\tilde{\dot{s}}_2\hat{s}_2\dot{s}_2 \qquad (22)\\
\overline{\mathrm{PCI}}(\mathbf{C}_i;s_d,\tilde{s}_d,\ldots) &= \frac{1}{4}\overline{\mathrm{SCI}}(\mathbf{C}_i;s_d,\tilde{s}_d,\ldots)-\frac{1}{4}\overline{\mathrm{SCI}}(\mathbf{C}_{2h};s_d,\tilde{s}_d,\ldots)\\
&\quad -\frac{1}{4}\overline{\mathrm{SCI}}(\mathbf{C}_{2h}';s_d,\tilde{s}_d,\ldots)-\frac{1}{4}\overline{\mathrm{SCI}}(\mathbf{C}_{2h}'';s_d,\tilde{s}_d,\ldots)\\
&\quad +\frac{1}{2}\overline{\mathrm{SCI}}(\mathbf{D}_{2h};s_d,\tilde{s}_d,\ldots)=0 \qquad (23)\\
\overline{\mathrm{PCI}}(\mathbf{C}_{2v};s_d,\tilde{s}_d,\ldots) &= \frac{1}{2}\overline{\mathrm{SCI}}(\mathbf{C}_{2v};s_d,\tilde{s}_d,\ldots)-\frac{1}{2}\overline{\mathrm{SCI}}(\mathbf{D}_{2h};s_d,\tilde{s}_d,\ldots)=0 \qquad (24)
\end{aligned}$$

$$\overline{\mathrm{PCI}}(\mathbf{C}'_{2v};s_d,\tilde{s}_d,\ldots) = \frac{1}{2}\overline{\mathrm{SCI}}(\mathbf{C}'_{2v};s_d,\tilde{s}_d,\ldots) - \frac{1}{2}\overline{\mathrm{SCI}}(\mathbf{D}_{2h};s_d,\tilde{s}_d,\ldots) = 0 \tag{25}$$

$$\begin{aligned}\overline{\mathrm{PCI}}(\mathbf{C}''_{2v};s_d,\tilde{s}_d,\ldots) &= \frac{1}{2}\overline{\mathrm{SCI}}(\mathbf{C}''_{2v};s_d,\tilde{s}_d,\ldots) - \frac{1}{2}\overline{\mathrm{SCI}}(\mathbf{D}_{2h};s_d,\tilde{s}_d,\ldots) \\ &= s_1\tilde{s}_2\hat{s}_2\hat{\tilde{s}}_2\dot{s}_1 + \tilde{s}_2\tilde{\tilde{s}}_2\hat{s}_2\dot{s}_1^2 \end{aligned} \tag{26}$$

$$\begin{aligned}\overline{\mathrm{PCI}}(\mathbf{C}_{2h};s_d,\tilde{s}_d,\ldots) &= \frac{1}{2}\overline{\mathrm{SCI}}(\mathbf{C}_{2h};s_d,\tilde{s}_d,\ldots) - \frac{1}{2}\overline{\mathrm{SCI}}(\mathbf{D}_{2h};s_d,\tilde{s}_d,\ldots) \\ &= \tilde{s}_2\tilde{\tilde{s}}_2\hat{s}_2\dot{s}_2 \end{aligned} \tag{27}$$

$$\overline{\mathrm{PCI}}(\mathbf{C}'_{2h};s_d,\tilde{s}_d,\ldots) = \frac{1}{2}\overline{\mathrm{SCI}}(\mathbf{C}'_{2h};s_d,\tilde{s}_d,\ldots) - \frac{1}{2}\overline{\mathrm{SCI}}(\mathbf{D}_{2h};s_d,\tilde{s}_d,\ldots) = 0 \tag{28}$$

$$\overline{\mathrm{PCI}}(\mathbf{C}''_{2h};s_d,\tilde{s}_d,\ldots) = \frac{1}{2}\overline{\mathrm{SCI}}(\mathbf{C}''_{2h};s_d,\tilde{s}_d,\ldots) - \frac{1}{2}\overline{\mathrm{SCI}}(\mathbf{D}_{2h};s_d,\tilde{s}_d,\ldots) = 0 \tag{29}$$

$$\overline{\mathrm{PCI}}(\mathbf{D}_2;s_d,\tilde{s}_d,\ldots) = \frac{1}{2}\overline{\mathrm{SCI}}(\mathbf{D}_2;s_d,\tilde{s}_d,\ldots) - \frac{1}{2}\overline{\mathrm{SCI}}(\mathbf{D}_{2h};s_d,\tilde{s}_d,\ldots) = 0 \tag{30}$$

$$\overline{\mathrm{PCI}}(\mathbf{D}_{2h};s_d,\tilde{s}_d,\ldots) = \overline{\mathrm{SCI}}(\mathbf{D}_{2h};s_d,\tilde{s}_d,\ldots) = 0 \tag{31}$$

When the edges contained in the orbits shown as Δ_a–Δ_f (Eqs. 4–9) are differentiated, the following inventory functions are obtained:

$$s_d = \mathrm{Z}_a, \quad \tilde{s}_d = \mathrm{Z}_b, \quad \tilde{\tilde{s}}_d = \mathrm{Z}_c, \quad \hat{s}_d = \mathrm{Z}_d, \quad \hat{\tilde{s}}_d = \mathrm{Z}_e, \quad \dot{s}_d = \mathrm{Z}_f. \tag{32}$$

Then, they are introduced into the RPCIs (Eqs. 16–31). The resulting equations are expanded to give the following generating functions:

$$f_{\mathbf{C}''_s} = 0 \tag{33}$$

$$f_{\mathbf{C}''_{2v}} = \mathrm{Z}_a\mathrm{Z}_b^2\mathrm{Z}_d^2\mathrm{Z}_e^2\mathrm{Z}_f + \mathrm{Z}_b^2\mathrm{Z}_c^2\mathrm{Z}_d^2\mathrm{Z}_f \qquad (= 2\mathrm{Z}^8) \tag{34}$$

$$f_{\mathbf{C}_{2h}} = \mathrm{Z}_b^2\mathrm{Z}_c^2\mathrm{Z}_d^2\mathrm{Z}_f^2 \qquad (= \mathrm{Z}^8) \tag{35}$$

where only non-zero RPCIs (Eqs. 22, 26, and 27) among Eqs. 16–31 are shown for the sake of page saving. When we place $\mathrm{Z} = \mathrm{Z}_a = \mathrm{Z}_b = \mathrm{Z}_c = \mathrm{Z}_d = \mathrm{Z}_e = \mathrm{Z}_f$, Eqs. 33–35 are degenerated into the data shown in respective pairs of parentheses. This treatment is alternatively accomplished by using degenerate inventory functions in place of Eq. 32 as follows:

$$s_d = \mathrm{Z}, \quad \tilde{s}_d = \mathrm{Z}, \quad \tilde{\tilde{s}}_d = \mathrm{Z}, \quad \hat{s}_d = \mathrm{Z}, \quad \hat{\tilde{s}}_d = \mathrm{Z}, \quad \dot{s}_d = \mathrm{Z}, \tag{36}$$

Furthermore, Eqs. 16–31 are rewritten by using simplified RSCIs collected in the rightmost column of Table 1 in place of the restricted SCIs collected in the full-RSCI column, where the inventory function $s_d = \mathrm{Z}$ is introduced into the resulting simplified PCIs.

Among the structures depicted in Fig. 2, three structures, i.e., **2a** (= **2b**), **3a** (= **3b**), and **4a** (= **4b**), should be selected as non-equivalent structures under the action of $\mathbf{D}_{2h}$.

2.2 Interpretation of RSCIs

In order to gain a hint to enumerate perfect matchings, let us consider the restricted SCIs (RSCIs) calculated for the pyrene skeleton, which are collected in the full-RSCI column of Table 1. It should be emphasized that the RSCI for each subgroup gives the number of fixed structures by introducing the inventory functions (Eq. 32).

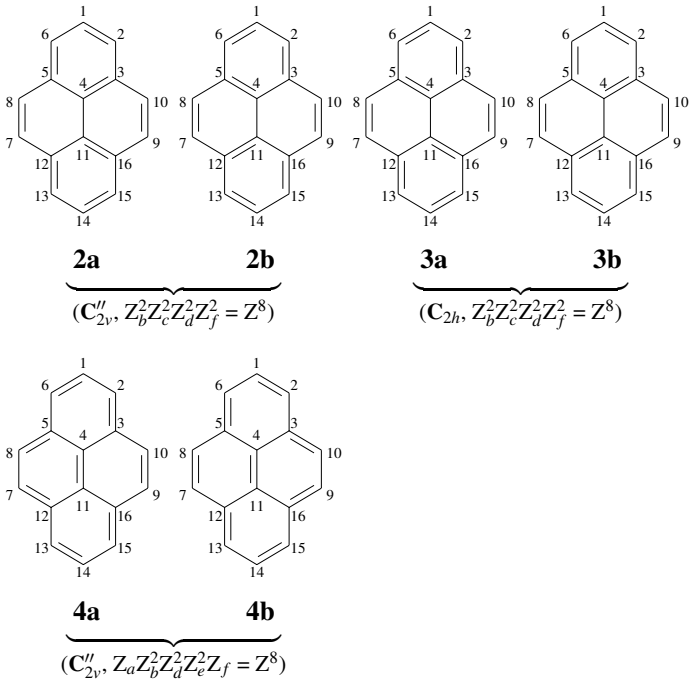

Figure 2: Fixed structures of pyrene on the action of $\mathbf{C}_1$ under the restriction condition. These correspond to a set of Kekulé structures, i.e., $K = 6$.

In particular, the RSCI for the $\mathbf{C}_1$-group represents a set of fully desymmetrized structures. For example, the data in the $\mathbf{C}_1$-row of Table 1 (or Eq. 15) gives the following generating function by introducing the inventory functions represented by Eq. 32:

$$g_{\mathbf{C}_1} = 2\mathrm{Z}_a\mathrm{Z}_b^2\mathrm{Z}_d^2\mathrm{Z}_e^2\mathrm{Z}_f + 4\mathrm{Z}_b^2\mathrm{Z}_c^2\mathrm{Z}_d^2\mathrm{Z}_f^2 \qquad (= 6\mathrm{Z}^8) \tag{37}$$

which corresponds to $6\mathrm{Z}^8$, when we place $\mathrm{Z} = \mathrm{Z}_a = \mathrm{Z}_b = \mathrm{Z}_c = \mathrm{Z}_d = \mathrm{Z}_e = \mathrm{Z}_f$. Because we use the inventory functions represented by Eq. 32, the data of Eq. 37 can be directly linked to the term $2s_1\tilde{s}^2\hat{s}_1^2\hat{\tilde{s}}_1^2\dot{s}_1 + 4\tilde{s}_1^2\tilde{\tilde{s}}_1^2\hat{s}_1^2\dot{s}_1^2$ as well as to the term $6s_1^8$, which are collected in the $\mathbf{C}_1$-row of Table 1. It is to be noted that each edge in the pyrene structure constructs one-membered orbit under the subgroup $\mathbf{C}_1$, so that the relevant sphericity index (SI) has a subscript 1, as found in a_1, b_1, and c_1 (or s_1 without chirality fittingness).

The term $2\mathrm{Z}_a\mathrm{Z}_b^2\mathrm{Z}_d^2\mathrm{Z}_e^2\mathrm{Z}_f$ (or $2s_1\tilde{s}^2\hat{s}_1^2\hat{\tilde{s}}_1^2\dot{s}_1$) indicates that there are two fixed structures represented by **4a** and **4b**, while the term $4\mathrm{Z}_b^2\mathrm{Z}_c^2\mathrm{Z}_d^2\mathrm{Z}_f^2$ (or $4\tilde{s}_1^2\tilde{\tilde{s}}_1^2\hat{s}_1^2\dot{s}_1^2$) indicates that there are four fixed structures represented by **2a**, **2b**, **3a**, and **3b**. The total power of each monomial is eight (as shown in s_1^8), which shows the presence of eight separate edges corresponding to conjugated double bonds. The number 16 of terminals corresponding to the eight edges is equal to the total number of vertices (16). It follows that the six fixed structures (Fig. 2) are perfect matchings of

pyrene, i.e., $K = 6$, where the symbol K represents the number of perfect matchings.

It should be noted that the total number 6 of the fixed structures appears as the sum of coefficients of the terms in Eq. 15 (the full RSCI at the $\mathbf{C}_1$-row of Table 1) or Eq. 37. In addition, the same number appears as the coefficient of the term s_1^8 (the simplified RSCI at the $\mathbf{C}_1$-row of Table 1). These facts provide us with keys to the development of the RSCI method for counting perfect matchings, as discussed in the following section.

3 Enumeration of Perfect Matchings

3.1 The RSCI Method for Counting Perfect Matchings

The above-mentioned discussions (Section 2) indicate that the RSCI for the $\mathbf{C}_1$-group is sufficient to examine perfect matchings.

Suppose that an orbit $\Delta_{i\alpha}$ (the α-th orbit governed by the coset representation $\mathbf{G}(/\mathbf{G}_i)$) in a given skeleton is fixed under the subgroup $\mathbf{C}_1$. Because the subduction into the $\mathbf{C}_1$-group divides the orbit into one-membered suborbits, the unit subduced cycle index (USCI) for an orbit $\Delta_{i\alpha}$, which is represented by $\mathrm{Z}(\mathbf{G}(/\mathbf{G}_i) \downarrow \mathbf{G}_j; s_{d_{jk}}^{(i\alpha)})$ (note $\mathbf{G}_j = \mathbf{C}_1$) in Eq. 1, is concluded to be

$$\mathrm{Z}(\mathbf{G}(/\mathbf{G}_i) \downarrow \mathbf{C}_1; s_{d_{jk}}^{(i\alpha)}) = (s_1^{(i\alpha)})^{|\mathbf{G}|/|\mathbf{G}_i|}. \tag{38}$$

Note that each $\mathbf{G}(/\mathbf{G}_i)$-orbit has a size of $|\mathbf{G}|/|\mathbf{G}_i|$ and divided into the number $|\mathbf{G}|/|\mathbf{G}_i|$ of one-membered suborbits during its subduction into $\mathbf{C}_1$. As for examples, see the USCIs for the orbits Δ_a–Δ_f collected in the $\mathbf{C}_1$-row of Table 1. Hence, Eq. 1 is converted into the following SCI for $\mathbf{C}_1$:

$$\mathrm{SCI}(\mathbf{C}_1; s_1^{(i\alpha)}) = \prod_{i=1}^{s} \prod_{\substack{\alpha=1 \\ \alpha_i \neq 0}}^{\alpha_i} \mathrm{Z}(\mathbf{G}(/\mathbf{G}_i) \downarrow \mathbf{C}_1; s_{d_{jk}}^{(i\alpha)}) = \prod_{i=1}^{s} \prod_{\substack{\alpha=1 \\ \alpha_i \neq 0}}^{\alpha_i} (s_1^{(i\alpha)})^{|\mathbf{G}|/|\mathbf{G}_i|}. \tag{39}$$

In order to apply Def. 1 to this case, each variable $s_1^{(i\alpha)}$ (for a one-membered suborbit), which is selected from the repeated multiplication $(s_1^{(i\alpha)})^{|\mathbf{G}|/|\mathbf{G}_i|}$ (for $\Delta_{i\alpha}$) in the right-hand side of Eq. 39, should be differentiated from the remaining one-membered suborbits and combined with a specific territory indicator (TI). When the suborbits are differentiated form one another by means of a superscript β, the corresponding TIs are represented by the symbol $t^{(i\alpha\beta)}(x_1, \ldots, x_v)$. Suppose that each of the one-membered suborbits contains an edge $\{k_\beta, l_\beta\}$ contained in the orbit $\Delta_{i\alpha}$. Then, the terminal vertices k_β and l_β of the edge produces a product of dummy variables $x_{k_\beta} x_{l_\beta}$ so that we obtain the following TI:

$$t^{(i\alpha\beta)}(x_1, \ldots, x_v) = x_{k_\beta} x_{l_\beta}. \tag{40}$$

It follows that the general definition of territory discriminants (Def. 1) is converted into a specific definition for the subgroup $\mathbf{C}_1$ as follows:

Definition 2 (Territory Discriminant for the Subgroup $\mathbf{C}_1$)

$$\mathrm{DSCI}(\mathbf{C}_1; s_1^{(i\alpha)}, x_1, x_2, \ldots, x_v) = \prod_{i=1}^{s} \prod_{\substack{\alpha=1 \\ \alpha_i \neq 0}}^{\alpha_i} \prod_{\beta=1}^{|\mathbf{G}|/|\mathbf{G}_i|} \left(1 + s_1^{(i\alpha)} t^{(i\alpha\beta)}(x_1, \ldots, x_v)\right). \tag{41}$$

The symbol $t^{(i\alpha\beta)}(x_1,\ldots,x_v)$ denotes a territory indicator (TI) of a one-membered suborbit at issue, as found in Eq. 40.

The expansion of Eq. 41 gives a set of candidate monomials (with TIs), among which monomials signified by a TI $x_1x_2\cdots x_v$ (in which each x_i appears only once) match the restriction condition and are necessary to construct a restricted SCI for $\mathbf{C}_1$. Lemma 1 is converted to meet a specific case as follows:

Lemma 2 (RSCI for the Subgroup $\mathbf{C}_1$) Among the monomials contained in the territory discriminant generated by Def. 1, monomials signified by the TI $x_1x_2\cdots x_v$ (in which each x_i appears only once) are selected by means of the following equation:

$$\overline{\mathrm{SCI}}(\mathbf{C}_1;s_1^{(i\alpha)}) = \frac{\partial^v}{\partial x_1\partial x_2\cdots\partial x_v}\mathrm{DSCI}(\mathbf{C}_1;s_1^{(i\alpha)},x_1,x_2,\ldots,x_v)\Bigg|_{x_1=x_2=\cdots=x_v=0}, \tag{42}$$

where the TI part of each selected monomial is replaced by 1 (no appearance).

As for an pyrene skeleton as an example, see Eq. 15.

Lemma 2 (Eq. 42) generates a polynomial which consists of several monomials represented as follows:

$$\prod_{i=1}^{s}\prod_{\substack{\alpha=1\\ \alpha_i\neq 0}}^{\alpha_i}(s_1^{(i\alpha)})^{z^{(i\alpha)}} \tag{43}$$

where the symbol $z^{(i\alpha)}$ represents the power of the variable $s_1^{(i\alpha)}$ corresponding to the orbit $\Delta_{i\alpha}$. The coefficient of the monomial (Eq. 43) in the polynomial generated by Eq. 42 is the number of fixed structures characterized by the monomial (Eq. 43). Compare Eq. 43 with Eq. 39. In general, we have $z^{(i\alpha)} < |\mathbf{G}|/|\mathbf{G}_i|$ because of the restriction condition. As for the first monomial $2s_1\tilde{s}_1^2\hat{s}_1^2\hat{\tilde{s}}_1^2\hat{s}_1$ in the right-hand side of Eq. 15, for example, the sphericity indices represented by s_1, $\tilde{s}_1$, etc. correspond to $s_1^{(i\alpha)}$ of Eq. 43 and their powers (1 for s_1, 2 for $\tilde{s}_1$, etc.) correspond to $z^{(i\alpha)}$ of Eq. 43. The coefficient 2 indicates the number of fixed structures.

The total power of the monomial (Eq. 43) is calculated to be

$$\sum_{i=1}^{s}\sum_{\substack{\alpha=1\\ \alpha_i\neq 0}}^{\alpha_i} z^{(i\alpha)}, \tag{44}$$

which indicates the number of edges corresponding to the monomial represented by Eq. 43. When the monomial (Eq. 43) corresponds to the perfect matchings, we should put

$$\frac{v}{2} = \sum_{i=1}^{s}\sum_{\substack{\alpha=1\\ \alpha_i\neq 0}}^{\alpha_i} z^{(i\alpha)}, \tag{45}$$

where v is the number of vertices contained in the skeleton of $\mathbf{G}$ at issue. The above-mentioned discussions are summarized into the following theorem.

Theorem 1 (Number of Perfect Matchings) The number of perfect matchings is the sum of the coefficients of the monomials (Eq. 43) which appear in the RSCI represented by Eq. 42, where the total power (Eq. 44) satisfies Eq. 45.

3.2 Simplified Procedures for Determining Perfect Matchings

Theorem 1 gives the number of perfect matchings which is divided into itemized values with respect to the orbits of edges governed by coset representations $\mathbf{G}(/\mathbf{G}_i)$. In most cases, however, such itemized values are unnecessary so that the sum described in Theorem 1 is desirable to be obtained directly. For this purpose, each edge is directly treated without considering the orbits $\Delta_{i\alpha}$ governed by $\mathbf{G}(/\mathbf{G}_i)$ as well as the subdivision into suborbits differentiated by β. The SCI for $\mathbf{C}_1$ (Eq. 39) is simplified into the following formula:

$$\mathrm{SCI}(\mathbf{C}_1; s_1) = s_1^e, \tag{46}$$

where e represents the number of edges. Because each edge constructs one-membered orbit under the action of $\mathbf{C}_1$, the territory discriminant for the subgroup $\mathbf{C}_1$ (Eq. 2) is simplified as follows to meet the present purpose.

Definition 3 (Simplified Territory Discriminant for the Subgroup $\mathbf{C}_1$) Let us consider a given graph which has v vertices and e edges. Suppose that each one-membered orbit of an edge $\{k_\beta, l_\beta\}$ (for $\beta = 1, 2, \ldots, e$) is examined to obtain perfect matchings. The territory indicator of the edge is defined as a product of dummy variables $x_{k_\beta} x_{l_\beta}$ on the basis of the terminal vertices k_β and l_β. A simplified territory discriminant of the subgroup $\mathbf{C}_1$ is defined by the following equation:

$$\mathrm{DSCI}(\mathbf{C}_1; s_1, x_1, x_2, \ldots, x_v) = \prod_{\beta=1}^{e} \left(1 + s_1 x_{k_\beta} x_{l_\beta}\right). \tag{47}$$

Lemma 2 is further simplified to meet the present purpose as follows:

Lemma 3 (Simplified RSCI for the Subgroup $\mathbf{C}_1$) Among the monomials contained in the territory discriminant generated by Def. 3, monomials signified by the TI $x_1 x_2 \cdots x_v$ (in which each x_i appears only once) are selected by means of the following equation:

$$\overline{\mathrm{SCI}}(\mathbf{C}_1; s_1) = \frac{\partial^v}{\partial x_1 \partial x_2 \cdots \partial x_v} \mathrm{DSCI}(\mathbf{C}_1; s_1, x_1, x_2, \ldots, x_v) \Bigg|_{x_1 = x_2 = \cdots = x_v = 0}, \tag{48}$$

where the TI part of each selected monomial is replaced by 1 (no appearance).

As for an pyrene skeleton as an example, see the right-most column in the $\mathbf{C}_1$-row of Table 1.

The simplified version of Theorem 1 is described as follows:

Theorem 2 (Simplified Method for Obtaining Number of Perfect Matchings) The number of perfect matchings is the coefficient of the monomial $s_1^{v/2}$ which appear in the simplified RSCI represented by Eq. 48, where v is the total number of vertices.

When any perfect matchings exist, the multiple partial differential due to Eq. 48 leaves one monomial only, because there is only one monomial containing the TI $x_1 x_2 \cdots x_v$.

4 Examples

After a practical calculation of the number of perfect matchings for a dodecahedral skeleton is shown by using the Maple programming language, several examples adopted from Chapter 8 of the textbook by Trinajstić [1] are examined to show the versatility of the RSCI method.

4.1 Dodecahedral Skeleton

As a dodecahedral skeleton, dodecahedrane is known as a fully saturated hydrocarbon [16]. Let us consider unsaturated derivatives with ten double bonds. They are regarded as perfect matchings of the dodecahedral skeleton, the vertices of which are numbered as shown in Fig. 3, i.e., a projection diagram (**5**) and a Schlegel diagram (**6**).

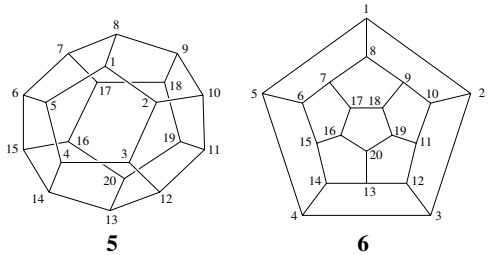

Figure 3: The numbering of a dodecahedron skeleton as a projection diagram (left) and a Schlegel diagram. $K = 36$.

According to Eq. 47 of Def. 3, the corresponding simplified territory discriminant is calculated as follows:

$$
\begin{aligned}
&\mathrm{DSCI}(\mathbf{C}_1; s_1, x_1, x_2, \ldots, x_{20}) = \\
&\quad (1+s_1x_1x_2)(1+s_1x_1x_5)(1+s_1x_1x_8)(1+s_1x_2x_3)(1+s_1x_2x_{10}) \\
&\quad \times(1+s_1x_3x_4)(1+s_1x_3x_{12})(1+s_1x_4x_5)(1+s_1x_4x_{14})(1+s_1x_5x_6) \\
&\quad \times(1+s_1x_6x_7)(1+s_1x_6x_{15})(1+s_1x_7x_8)(1+s_1x_7x_{17})(1+s_1x_8x_9) \\
&\quad \times(1+s_1x_9x_{10})(1+s_1x_9x_{18})(1+s_1x_{10}x_{11})(1+s_1x_{11}x_{12})(1+s_1x_{11}x_{19}) \\
&\quad \times(1+s_1x_{12}x_{13})(1+s_1x_{13}x_{14})(1+s_1x_{13}x_{20})(1+s_1x_{14}x_{15})(1+s_1x_{15}x_{16}) \\
&\quad \times(1+s_1x_{16}x_{17})(1+s_1x_{16}x_{20})(1+s_1x_{17}x_{18})(1+s_1x_{18}x_{19})(1+s_1x_{19}x_{20}). \qquad (49)
\end{aligned}
$$

The simplified territory discriminant (Eq. 49) for the dodecahedral skeleton (**5**) is expanded and treated by means of Lemma 3. Direct applications of Eq. 48 of Lemma 3 sometimes encounter combinatorial explosion due to a shortage of computer memories. To avoid such explosion in a practical calculation, such a simplified territory discriminant as Eq. 49 is divided into several parts, which are treated successively as exemplified in the following Maple program (named "dodecahedrane.mpl"):

```
#dodecahedrane.mpl
DSCIC1A :=
(1+s1*x1*x2)*(1+s1*x1*x5)*(1+s1*x1*x8)*
(1+s1*x2*x3)*(1+s1*x2*x10)*
(1+s1*x3*x4)*(1+s1*x3*x12)*
(1+s1*x4*x5)*(1+s1*x4*x14)*
(1+s1*x5*x6)*
(1+s1*x6*x7)*(1+s1*x6*x15);

DSCIC1B :=
(1+s1*x7*x8)*(1+s1*x7*x17)*
(1+s1*x8*x9)*
(1+s1*x9*x10)*(1+s1*x9*x18)*
(1+s1*x10*x11)*
```

```
(1+s1*x11*x12)*(1+s1*x11*x19)*
(1+s1*x12*x13);

DSCIC1C :=
(1+s1*x13*x14)*(1+s1*x13*x20)*
(1+s1*x14*x15)*
(1+s1*x15*x16)*
(1+s1*x16*x17)*(1+s1*x16*x20)*
(1+s1*x17*x18)*
(1+s1*x18*x19)*
(1+s1*x19*x20);

tempC1A := expand(DSCIC1A):
tempC1B := diff(tempC1A, x1,x2,x3,x4,x5,x6):
x1 :=0; x2 :=0; x3 :=0; x4 :=0;
x5 :=0; x6 :=0;
tempC1C := expand(tempC1B);

tempC1A := expand(tempC1C*DSCIC1B):
tempC1B := diff(tempC1A, x7,x8,x9,
x10,x11,x12):
x7 :=0; x8 :=0; x9 :=0; x10 :=0;
x11 :=0; x12 :=0;
tempC1C := expand(tempC1B);

tempC1A := expand(tempC1C*DSCIC1C):
tempC1B := diff(tempC1A, x13,x14,x15,x16,
x17,x18,x19,x20):
x13 :=0; x14:=0; x15 :=0; x16 :=0;
x17 :=0; x18 :=0; x19 :=0; x20 :=0;
tempC1C := expand(tempC1B);
```

The territory discriminant is tentatively divided into three parts (`DSCIC1A`, `DSCIC1B`, and `DSCIC1D`) in the above program. Such a mode of division is arbitrary so long as the capacity of computer memories allows. The result due to the last line (`tempC1C`) gives the following simplified RSCI:

$$\overline{\mathrm{SCI}}(\mathbf{C}_1;s_1) = 36s_1^{10}. \tag{50}$$

Hence, Theorem 2 teaches us that the coefficient 36 of the monomial s_1^{10} ($v = 20$ for **5**) indicates the number of perfect matchings (i.e., the number of Kekulé structures, $K = 36$) for the dodecahedral skeleton (**5**).

4.2 Coronene

Enumerations of Kekulé structures of coronene by the fragmentation method (Fig. 6 of [1]) and by the method based on the lattice structures of fused benzenoids (Fig.15 of [1]) have been reported as shown in the textbook [1]. In order to apply Theorem 2 to the coronene skeleton (**7**), the numbering shown in Fig. 4 is adopted, although the mode of numbering can be selected arbitrarily without losing generality.

According to Def. 3, the simplified territory discriminant corresponding to the numbering shown in Fig. 4 is obtained as follows:

$$\begin{aligned}
&\mathrm{DSCI}(\mathbf{C}_1;s_1,x_1,x_2,\ldots,x_{24}) = \\
&\quad (1+s_1x_1x_2)(1+s_1x_1x_{18})(1+s_1x_2x_{13})(1+s_1x_3x_4)(1+s_1x_3x_{13}) \\
&\quad \times(1+s_1x_4x_{14})(1+s_1x_5x_6)(1+s_1x_5x_{14})(1+s_1x_6x_{15})(1+s_1x_7x_8) \\
&\quad \times(1+s_1x_7x_{15})(1+s_1x_8x_{16})(1+s_1x_9x_{10})(1+s_1x_9x_{16})(1+s_1x_{10}x_{17}) \\
&\quad \times(1+s_1x_{11}x_{12})(1+s_1x_{11}x_{17})(1+s_1x_{12}x_{18})(1+s_1x_{13}x_{19})(1+s_1x_{14}x_{20}) \\
&\quad \times(1+s_1x_{15}x_{21})(1+s_1x_{16}x_{22})(1+s_1x_{17}x_{23})(1+s_1x_{18}x_{24})(1+s_1x_{19}x_{20}) \\
&\quad \times(1+s_1x_{20}x_{21})(1+s_1x_{21}x_{22})(1+s_1x_{22}x_{23})(1+s_1x_{23}x_{24})(1+s_1x_{24}x_{19}).
\end{aligned} \tag{51}$$

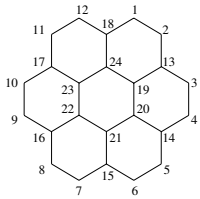

7

Figure 4: Numbering of a Coronene Skeleton. $K = 20$.

The simplified territory discriminant (Eq. 51) for the coronene skeleton (**7**) is divided into three parts so as to be expanded and treated successively by means of Lemma 3. Thereby, the simplified RSCI is obtained as follows:

$$\overline{\mathrm{SCI}}(\mathbf{C}_1; s_1) = 20 s_1^{12}. \tag{52}$$

Hence, Theorem 2 shows that the coefficient 20 of the monomial s_1^{12} ($v = 24$ for **7**) is the number of perfect matchings (i.e., the number of Kekulé structures, $K = 20$) for the coronene skeleton (**7**). This value is identical with those reported previously by the fragmentation method (Fig. 6 of [1]) and by the method based on lattice structures (Fig.15 of [1]).

4.3 Dibenzo[b,n]picene

Enumerations of Kekulé structures of dibenzo[b,n]picene by the Gordon-Davidson method (Fig. 10 of [1]) and by the numeral-in-hexagon method (Fig.11 of [1]) have been reported as shown in the textbook [1]. The numbering shown in Fig. 5 is adopted in order to apply Theorem 2 to the dibenzo[b,n]picene skeleton (**8**).

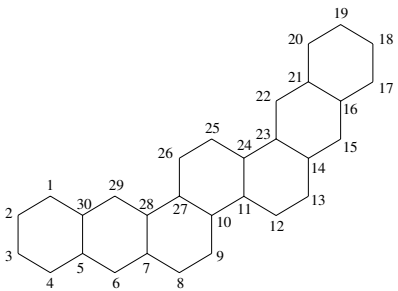

8

Figure 5: Numbering of a Dibenzo[b,n]picene Skeleton. $K = 25$.

The simplified territory discriminant corresponding to the numbering shown in Fig. 5 is

obtained according to Def. 3:

$$
\begin{aligned}
&\mathrm{DSCI}(\mathbf{C}_1; s_1, x_1, x_2, \ldots, x_{30}) = \\
&\quad (1+s_1x_1x_2)(1+s_1x_1x_{30})(1+s_1x_2x_3)(1+s_1x_3x_4)(1+s_1x_4x_5) \\
&\quad \times(1+s_1x_5x_6)(1+s_1x_5x_{30})(1+s_1x_6x_7)(1+s_1x_7x_8)(1+s_1x_7x_{28}) \\
&\quad \times(1+s_1x_8x_9)(1+s_1x_9x_{10})(1+s_1x_{10}x_{11})(1+s_1x_{10}x_{27})(1+s_1x_{11}x_{12}) \\
&\quad \times(1+s_1x_{11}x_{24})(1+s_1x_{12}x_{13})(1+s_1x_{13}x_{14})(1+s_1x_{14}x_{15})(1+s_1x_{14}x_{23}) \\
&\quad \times(1+s_1x_{15}x_{16})(1+s_1x_{16}x_{17})(1+s_1x_{16}x_{21})(1+s_1x_{17}x_{18})(1+s_1x_{18}x_{19}) \\
&\quad \times(1+s_1x_{19}x_{20})(1+s_1x_{20}x_{21})(1+s_1x_{21}x_{22})(1+s_1x_{22}x_{23}) \\
&\quad \times(1+s_1x_{23}x_{24})(1+s_1x_{24}x_{25})(1+s_1x_{25}x_{26})(1+s_1x_{26}x_{27}) \\
&\quad \times(1+s_1x_{27}x_{28})(1+s_1x_{28}x_{29})(1+s_1x_{29}x_{30}). \qquad (53)
\end{aligned}
$$

The simplified territory discriminant (Eq. 53) for dibenzo[b,n]picene (**8**) is divided into four parts so as to be expanded and treated successively by means of Lemma 3. Thereby, the simplified RSCI is obtained as follows:

$$\overline{\mathrm{SCI}}(\mathbf{C}_1; s_1) = 25 s_1^{15}. \qquad (54)$$

Hence, Theorem 2 teaches us that the coefficient 25 of the monomial s_1^{15} ($v = 30$ for **8**) indicates the number of perfect matchings (i.e., the number of Kekulé structures, $K = 25$) for the skeleton (**8**). This value is identical with those reported previously by the Gordon-Davidson method (Fig. 10 of [1]) and by the numeral-in-hexagon method (Fig.11 of [1]).

4.4 Dibenzo[bc,mn]ovalene

Enumerations of Kekulé structures of dibenzo[b,n]picene by the method of Yen (Fig. 14 of [1]) and by the numeral-in-hexagon method (Fig.18 of [1]) have been reported as shown in the textbook [1]. The numbering shown in Fig. 6 is adopted in order to apply Theorem 2 to the dibenzo[bc,mn]ovalene skeleton (**9**).

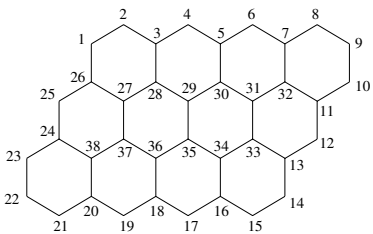

9

Figure 6: Numbering of a Dibenzo[bc,mn]ovalene Skeleton. $K = 35$.

According to Def. 3, the simplified territory discriminant corresponding to the numbering shown in Fig. 6 is obtained as follows:

$$\mathrm{DSCI}(\mathbf{C}_1; s_1, x_1, x_2, \ldots, x_{38}) =$$

$$
\begin{aligned}
&(1+s_1x_1x_2)(1+s_1x_1x_{26})(1+s_1x_2x_3)(1+s_1x_3x_4)(1+s_1x_3x_{28})\\
&\times(1+s_1x_4x_5)(1+s_1x_5x_6)(1+s_1x_5x_{30})(1+s_1x_6x_7)(1+s_1x_7x_8)\\
&\times(1+s_1x_7x_{32})(1+s_1x_8x_9)(1+s_1x_9x_{10})(1+s_1x_{10}x_{11})(1+s_1x_{11}x_{12})\\
&\times(1+s_1x_{11}x_{32})(1+s_1x_{12}x_{13})(1+s_1x_{13}x_{14})(1+s_1x_{13}x_{33})(1+s_1x_{14}x_{15})\\
&\times(1+s_1x_{15}x_{16})(1+s_1x_{16}x_{17})(1+s_1x_{16}x_{34})(1+s_1x_{17}x_{18})(1+s_1x_{18}x_{19})\\
&\times(1+s_1x_{18}x_{36})(1+s_1x_{19}x_{20})(1+s_1x_{20}x_{21})(1+s_1x_{20}x_{38})(1+s_1x_{21}x_{22})\\
&\times(1+s_1x_{22}x_{23})(1+s_1x_{23}x_{24})(1+s_1x_{24}x_{25})(1+s_1x_{24}x_{38})(1+s_1x_{25}x_{26})\\
&\times(1+s_1x_{26}x_{27})(1+s_1x_{27}x_{28})(1+s_1x_{27}x_{37})(1+s_1x_{28}x_{29})(1+s_1x_{29}x_{30})\\
&\times(1+s_1x_{29}x_{35})(1+s_1x_{30}x_{31})(1+s_1x_{31}x_{32})(1+s_1x_{31}x_{33})(1+s_1x_{33}x_{34})\\
&\times(1+s_1x_{34}x_{35})(1+s_1x_{35}x_{36})(1+s_1x_{36}x_{37})(1+s_1x_{37}x_{38}).
\end{aligned}
\tag{55}
$$

The simplified territory discriminant (Eq. 55) for dibenzo[bc,mn]ovalene (**9**) is divided into four parts. They are expanded and treated successively by means of Lemma 3. Thereby, the simplified RSCI is obtained as follows:

$$\overline{\mathrm{SCI}}(\mathbf{C}_1;s_1) = 35s_1^{19}. \tag{56}$$

By virtue of Theorem 2, the coefficient 35 of the monomial s_1^{19} ($v = 38$ for **9**) indicates the number of perfect matchings (i.e., the number of Kekulé structures, $K = 35$) for the skeleton (**9**). This value is identical with those reported previously by the method based on the lattice structures (Fig. 14 of [1]) and by the numeral-in-hexagon method (Fig.18 of [1]).

4.5 Dibenzo[fg,op]anthanthrene

Enumeration of Kekulé structures of dibenzo[fg,op]anthanthrene by the method of Yen (Fig. 16 of [1]) has been reported as shown in the textbook [1]. The numbering shown in Fig. 7 is adopted in order to apply Theorem 2 to the skeleton (**10**).

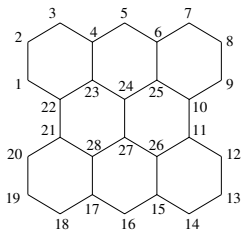

10

Figure 7: Numbering of a Dibenzo[fg,op]anthanthrene Skeleton. $K = 16$.

The simplified territory discriminant corresponding to the numbering shown in Fig. 7 is obtained as follows by virtue of Def. 3:

$$
\begin{aligned}
&\mathrm{DSCI}(\mathbf{C}_1;s_1,x_1,x_2,\ldots,x_{28}) =\\
&\quad(1+s_1x_1x_2)(1+s_1x_1x_{22})(1+s_1x_2x_3)(1+s_1x_3x_4)(1+s_1x_4x_5)
\end{aligned}
$$

$$\begin{aligned}
&\times(1+s_1x_4x_{23})(1+s_1x_5x_6)(1+s_1x_6x_7)(1+s_1x_6x_{25})(1+s_1x_7x_8)\\
&\times(1+s_1x_8x_9)(1+s_1x_9x_{10})(1+s_1x_{10}x_{11})(1+s_1x_{10}x_{25})(1+s_1x_{11}x_{12})\\
&\times(1+s_1x_{11}x_{26})(1+s_1x_{12}x_{13})(1+s_1x_{13}x_{14})(1+s_1x_{14}x_{15})(1+s_1x_{15}x_{16})\\
&\times(1+s_1x_{15}x_{26})(1+s_1x_{16}x_{17})(1+s_1x_{17}x_{18})(1+s_1x_{17}x_{28})(1+s_1x_{18}x_{19})\\
&\times(1+s_1x_{19}x_{20})(1+s_1x_{20}x_{21})(1+s_1x_{21}x_{22})(1+s_1x_{21}x_{28})(1+s_1x_{22}x_{23})\\
&\times(1+s_1x_{23}x_{24})(1+s_1x_{24}x_{25})(1+s_1x_{24}x_{27})(1+s_1x_{26}x_{27})(1+s_1x_{27}x_{28}). \qquad (57)
\end{aligned}$$

The simplified territory discriminant (Eq. 57) for dibenzo[fg,op]anthanthrene (**10**) is divided into four parts, which are expanded and treated successively by means of Lemma 3. Thereby, the simplified RSCI is obtained as follows:

$$\overline{\mathrm{SCI}}(\mathbf{C}_1;s_1) = 16s_1^{14}. \qquad (58)$$

By virtue of Theorem 2, the coefficient 16 of the monomial s_1^{14} ($v = 28$ for **9**) indicates the number of perfect matchings (i.e., the number of Kekulé structures, $K = 28$) for the skeleton (**10**). This value is identical with the value reported previously by the method of Yen (Fig. 16 of [1]).

4.6 Dibenze[hi,sl]ovalene

Enumeration of Kekulé structures of dibenze[hi,sl]ovalene by the path counting method (Fig. 24 of [1]) has been reported as shown in the textbook [1]. The numbering shown in Fig. 8 is adopted in order to apply Theorem 2 to the skeleton (**11**).

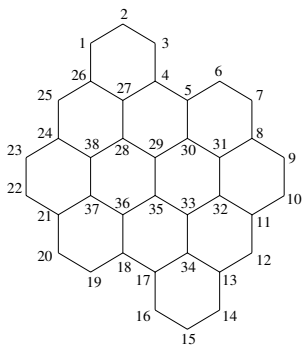

11

Figure 8: Numbering of a Dibenzo[hi,sl]ovalene Skeleton. $K = 85$.

By virtue of Def. 3, the simplified territory discriminant corresponding to the numbering shown in Fig. 8 is obtained as follows:

$$\begin{aligned}
&\mathrm{DSCI}(\mathbf{C}_1;s_1,x_1,x_2,\ldots,x_{38}) =\\
&\quad(1+s_1x_1x_2)(1+s_1x_1x_{26})(1+s_1x_2x_3)(1+s_1x_3x_4)(1+s_1x_4x_5)
\end{aligned}$$

$$
\begin{aligned}
&\times(1+s_1x_4x_{27})(1+s_1x_5x_6)(1+s_1x_5x_{30})(1+s_1x_6x_7)(1+s_1x_7x_8)\\
&\times(1+s_1x_8x_9)(1+s_1x_8x_{31})(1+s_1x_9x_{10})(1+s_1x_{10}x_{11})(1+s_1x_{11}x_{12})\\
&\times(1+s_1x_{11}x_{32})(1+s_1x_{12}x_{13})(1+s_1x_{13}x_{14})(1+s_1x_{13}x_{34})(1+s_1x_{14}x_{15})\\
&\times(1+s_1x_{15}x_{16})(1+s_1x_{16}x_{17})(1+s_1x_{17}x_{18})(1+s_1x_{17}x_{34})(1+s_1x_{18}x_{19})\\
&\times(1+s_1x_{18}x_{36})(1+s_1x_{19}x_{20})(1+s_1x_{20}x_{21})(1+s_1x_{21}x_{22})(1+s_1x_{21}x_{37})\\
&\times(1+s_1x_{22}x_{23})(1+s_1x_{23}x_{24})(1+s_1x_{24}x_{25})(1+s_1x_{24}x_{38})(1+s_1x_{25}x_{26})\\
&\times(1+s_1x_{26}x_{27})(1+s_1x_{27}x_{28})(1+s_1x_{28}x_{29})(1+s_1x_{28}x_{38})(1+s_1x_{29}x_{30})\\
&\times(1+s_1x_{29}x_{35})(1+s_1x_{30}x_{31})(1+s_1x_{31}x_{32})(1+s_1x_{32}x_{33})(1+s_1x_{33}x_{34})\\
&\times(1+s_1x_{33}x_{35})(1+s_1x_{35}x_{36})(1+s_1x_{36}x_{37})(1+s_1x_{37}x_{38}). \qquad (59)
\end{aligned}
$$

The simplified territory discriminant (Eq. 59) for dibenzo[hi,sl]ovalene (**11**) is divided into five parts. They are expanded and treated successively by means of Lemma 3. Thereby, the simplified RSCI is obtained as follows:

$$\overline{\mathrm{SCI}}(\mathbf{C}_1;s_1) = 85s_1^{19}. \qquad (60)$$

Theorem 2 shows that the coefficient 85 of the monomial s_1^{19} ($v = 38$ for **11**) indicates the number of perfect matchings (i.e., the number of Kekulé structures, $K = 85$) for the skeleton (**11**). This value is identical with the value reported previously by the path counting method (Fig. 24 of [1]).

4.7 Naphtho[8,1,2-efg]anthanthrene

Enumeration of Kekulé structures of naphtho[8,1,2-efg]anthanthrene by the matrix method of Hall (Fig. 25 of [1]) has been reported as shown in the textbook [1]. The numbering shown in Fig. 9 is adopted in order to apply Theorem 2 to the skeleton (**12**).

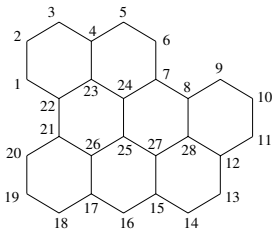

12

Figure 9: Numbering of a Naphtho[8,1,2-efg]anthanthrene Skeleton. $K = 26$.

By applying Def. 3 to the numbering shown in Fig. 9, the corresponding simplified territory discriminant is obtained as follows:

$$
\begin{aligned}
&\mathrm{DSCI}(\mathbf{C}_1;s_1,x_1,x_2,\ldots,x_{28}) =\\
&\quad(1+s_1x_1x_2)(1+s_1x_1x_{22})(1+s_1x_2x_3)(1+s_1x_3x_4)(1+s_1x_4x_5)\\
&\quad\times(1+s_1x_4x_{23})(1+s_1x_5x_6)(1+s_1x_6x_7);(1+s_1x_7x_8)(1+s_1x_7x_{24})
\end{aligned}
$$

$$\times(1+s_1x_8x_9)(1+s_1x_8x_{28})(1+s_1x_9x_{10})(1+s_1x_{10}x_{11})(1+s_1x_{11}x_{12})$$
$$\times(1+s_1x_{12}x_{13})(1+s_1x_{12}x_{28})(1+s_1x_{13}x_{14})(1+s_1x_{14}x_{15})(1+s_1x_{15}x_{16})$$
$$\times(1+s_1x_{15}x_{27})(1+s_1x_{16}x_{17})(1+s_1x_{17}x_{18})(1+s_1x_{17}x_{26})(1+s_1x_{18}x_{19})$$
$$\times(1+s_1x_{19}x_{20})(1+s_1x_{20}x_{21})(1+s_1x_{21}x_{22})(1+s_1x_{21}x_{26})(1+s_1x_{22}x_{23})$$
$$\times(1+s_1x_{23}x_{24})(1+s_1x_{24}x_{25})(1+s_1x_{25}x_{26})(1+s_1x_{25}x_{27})(1+s_1x_{27}x_{28}). \tag{61}$$

The simplified territory discriminant (Eq. 61) for naphtho[8,1,2-efg]anthanthrene (**12**) is divided into four parts. They are expanded and treated successively by means of Lemma 3. Thereby, the simplified RSCI is obtained as follows:

$$\overline{\mathrm{SCI}}(\mathbf{C}_1;s_1) = 26s_1^{14}. \tag{62}$$

It follows that the coefficient 26 of the monomial s_1^{14} ($v = 28$ for **12**) indicates the number of perfect matchings (i.e., the number of Kekulé structures, $K = 26$) for the skeleton (**12**) by using Theorem 2. This value is identical with the value reported previously by the matrix method of Hall (Fig. 25 of [1]).

4.8 Fullerene C_{60}

Enumerations of Kekulé structures of fullerene C_{60} by the Z-counting polynomial method [12] and by the transfer-matrix method [11] have been reported. The numbering shown in Fig. 10 is adopted in order to apply Theorem 1 and Theorem 2 to the skeleton (**13**).

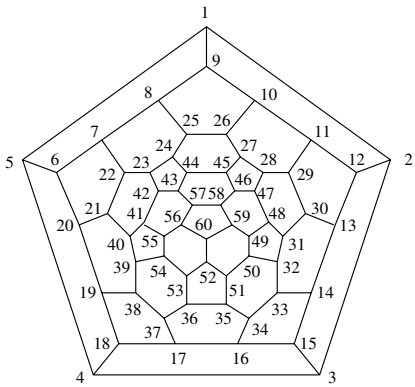

13

Figure 10: Numbering of a Fullerene C_{60} Skeleton (Schlegel diagram). $K = 12500$.

The thirty [6:6]-edges and the sixty [5:6]-edges are distinguished by the dummy variables s_1 and $\tilde{s}_1$. By applying Def. 2 to the numbering shown in Fig. 10, the corresponding territory discriminant is obtained as follows:

$$\mathrm{DSCI}(\mathbf{C}_1;s_1,\tilde{s}_1,x_1,x_2,\ldots,x_{60}) =$$

$$
\begin{aligned}
&(1+\tilde{s}_1x_1x_2)(1+\tilde{s}_1x_1x_5)(1+s_1x_1x_9)(1+\tilde{s}_1x_2x_3)(1+s_1x_2x_{12})\\
&\times(1+\tilde{s}_1x_3x_4)(1+s_1x_3x_{15})(1+\tilde{s}_1x_4x_5)(1+s_1x_4x_{18})(1+s_1x_5x_6)\\
&\times(1+\tilde{s}_1x_6x_7)(1+\tilde{s}_1x_6x_{20})(1+s_1x_7x_8)(1+\tilde{s}_1x_7x_{22})(1+\tilde{s}_1x_8x_9)\\
&\times(1+\tilde{s}_1x_8x_{25})(1+\tilde{s}_1x_9x_{10})(1+s_1x_{10}x_{11})(1+\tilde{s}_1x_{10}x_{26})(1+\tilde{s}_1x_{11}x_{12})\\
&\times(1+\tilde{s}_1x_{11}x_{29})(1+\tilde{s}_1x_{12}x_{13})(1+s_1x_{13}x_{14})(1+\tilde{s}_1x_{13}x_{30})(1+\tilde{s}_1x_{14}x_{15})\\
&\times(1+\tilde{s}_1x_{14}x_{33})(1+\tilde{s}_1x_{15}x_{16})(1+s_1x_{16}x_{17})(1+\tilde{s}_1x_{16}x_{34})(1+\tilde{s}_1x_{17}x_{18})\\
&\times(1+\tilde{s}_1x_{17}x_{37})(1+\tilde{s}_1x_{18}x_{19})(1+s_1x_{19}x_{20})(1+\tilde{s}_1x_{19}x_{38})(1+\tilde{s}_1x_{20}x_{21})\\
&\times(1+\tilde{s}_1x_{21}x_{22})(1+s_1x_{21}x_{40})(1+s_1x_{22}x_{23})(1+\tilde{s}_1x_{23}x_{24})(1+\tilde{s}_1x_{23}x_{42})\\
&\times(1+s_1x_{24}x_{25})(1+\tilde{s}_1x_{24}x_{44})(1+\tilde{s}_1x_{25}x_{26})(1+s_1x_{26}x_{27})(1+\tilde{s}_1x_{27}x_{28})\\
&\times(1+\tilde{s}_1x_{27}x_{45})(1+s_1x_{28}x_{29})(1+\tilde{s}_1x_{28}x_{47})(1+\tilde{s}_1x_{29}x_{30})(1+s_1x_{30}x_{31})\\
&\times(1+\tilde{s}_1x_{31}x_{32})(1+\tilde{s}_1x_{31}x_{48})(1+s_1x_{32}x_{33})(1+\tilde{s}_1x_{32}x_{50})(1+\tilde{s}_1x_{33}x_{34})\\
&\times(1+s_1x_{34}x_{35})(1+\tilde{s}_1x_{35}x_{36})(1+\tilde{s}_1x_{35}x_{51})(1+s_1x_{36}x_{37})(1+\tilde{s}_1x_{36}x_{53})\\
&\times(1+\tilde{s}_1x_{37}x_{38})(1+s_1x_{38}x_{39})(1+\tilde{s}_1x_{39}x_{40})(1+\tilde{s}_1x_{39}x_{54})(1+\tilde{s}_1x_{40}x_{41})\\
&\times(1+\tilde{s}_1x_{41}x_{55})(1+s_1x_{41}x_{42})(1+\tilde{s}_1x_{42}x_{43})(1+\tilde{s}_1x_{43}x_{44})(1+s_1x_{43}x_{57})\\
&\times(1+s_1x_{44}x_{45})(1+\tilde{s}_1x_{45}x_{46})(1+\tilde{s}_1x_{46}x_{47})(1+s_1x_{46}x_{58})(1+s_1x_{47}x_{48})\\
&\times(1+\tilde{s}_1x_{48}x_{49})(1+\tilde{s}_1x_{49}x_{50})(1+s_1x_{49}x_{59})(1+s_1x_{50}x_{51})(1+\tilde{s}_1x_{51}x_{52})\\
&\times(1+\tilde{s}_1x_{52}x_{53})(1+s_1x_{52}x_{60})(1+s_1x_{53}x_{54})(1+\tilde{s}_1x_{54}x_{55})(1+s_1x_{55}x_{56})\\
&\times(1+\tilde{s}_1x_{56}x_{57})(1+\tilde{s}_1x_{56}x_{60})(1+\tilde{s}_1x_{57}x_{58})(1+\tilde{s}_1x_{58}x_{59})(1+\tilde{s}_1x_{59}x_{60}). \qquad (63)
\end{aligned}
$$

To avoid combinatorial explosion, the territory discriminant (Eq. 63) for fullerene C_{60} (**13**) is divided into ten parts tentatively during a practical calculation. They are expanded and treated successively by means of Lemma 2. Thereby, the RSCI is obtained as follows:

$$
\begin{aligned}
&\overline{\mathrm{SCI}}(\mathbf{C}_1;s_1,\tilde{s}_1) =\\
&\quad s_1^{30}+20s_1^{27}\tilde{s}_1^{3}+160s_1^{24}\tilde{s}_1^{6}+660s_1^{21}\tilde{s}_1^{9}+36s_1^{20}\tilde{s}_1^{10}+1510s_1^{18}\tilde{s}_1^{12}+360s_1^{17}\tilde{s}_1^{13}\\
&\quad +1972s_1^{15}\tilde{s}_1^{15}+1260s_1^{14}\tilde{s}_1^{16}+120s_1^{13}\tilde{s}_1^{17}+1560s_1^{12}\tilde{s}_1^{18}+1800s_1^{11}\tilde{s}_1^{19}\\
&\quad +636s_1^{10}\tilde{s}_1^{20}+660s_1^{9}\tilde{s}_1^{21}+1020s_1^{8}\tilde{s}_1^{22}+600s_1^{7}\tilde{s}_1^{23}+125s_1^{6}\tilde{s}_1^{24}, \qquad (64)
\end{aligned}
$$

where the coefficient of each monomial $s_1^n\tilde{s}_1^{n'}$ $(n+n'=30)$ indicates the number of perfect matchings with n of [6:6]-edges and n' of [5:6]-edges. The sum of these coefficients is calculated to be 12500, which is the number of perfect matchings, as indicated by Theorem 1.

By putting $\tilde{s}_1 = s_1$, the territory discriminant (Eq. 63) can be converted into a simplified territory discriminant, which is also divided into ten parts so as to be expanded and treated successively by means of Lemma 3. Thereby, the simplified RSCI is obtained as follows:

$$
\overline{\mathrm{SCI}}(\mathbf{C}_1;s_1) = 12500s_1^{30}, \qquad (65)
$$

which is alternatively obtained by putting $\tilde{s}_1 = s_1$ in Eq. 64. Hence, the coefficient 12500 of the monomial s_1^{30} ($v = 60$ for **13**) indicates the number of perfect matchings (i.e., the number of Kekulé structures, $K = 12500$) for the skeleton (**12**) by using Theorem 2. This value is identical with those reported previously by the Z-counting polynomial method [12] and by the transfer-matrix method [11].

5 Conclusion

Restricted enumerations based on the USCI approach are discussed from a viewpoint of subductions into the $\mathbf{C}_1$-group, where we take account of edges contained in a given skeleton. Thereby, the restricted-subduced-cycle-index (RSCI) method for enumerating Kekulé structures has been developed as a specialized application of the USCI approach.

References

[1] N. Trinajstić, "Chemical Graph Theory," 2nd ed., CRC Press, Boca Raton (1992).

[2] M. Randić, *J. Chem. Soc. Faraday Trans. II*, **72**, 232 (1976).

[3] G. W. Wheland, *J. Chem. Phys.*, **3**, 356 (1933).

[4] A. Graovac, I. Gutman, N. Trinajstić, and T. Živković, *Theor. Chim. Acta*, **26**, 67 (1972).

[5] M. Gordon and W. H. Davidson, *J. Chem. Phys.*, **20**, 428 (1952).

[6] S. J. Cyvin and I. Gutman, "Kekulé Structures in Benzenoid Hydrocarbons," Springer Verlag, Berlin (1988).

[7] S. J. Cyvin and I. Gutman, *Math. Chem. (Mülheim/Ruhr)*, **19**, 229 (1986).

[8] T. F. Yen, *Theor. Chim. Acta*, **20**, 399 (1971).

[9] H. Sachs, *Combinatorica*, **4**, 89 (1984).

[10] G. G. Hall, *Chem. Phys. Lett.*, **145**, 168 (1988).

[11] D. J. Klein, T. G. Schmalz, G. E. Hite, and W. A. Seitz, *J. Am. Chem. Soc.*, **108**, 203 (1986).

[12] H. Hosoya, *Comp. Math. with Appls.*, **12B**, 271 (1986).

[13] S. Fujita, "Symmetry and Combinatorial Enumeration in Chemistry," Springer-Verlag, Berlin-Heidelberg (1991).

[14] S. Fujita, *Tetrahedron*, **46**, 365–382 (1990).

[15] M. B. Monagan, K. O. Geddes, K. M. Heal, G. Labahn, S. M. Vorkoetter, J. McCarron, and P. DeMarco, "Maple 9. Advanced Programming Guide," Maplesoft, Waterloo (2003).

[16] L. A. Paquette, *Chem. Rev.*, **89**, 1051–1065 (1989).